Available online at www.sciencedirect.com
SCIENCE DIRECT
Polymer 46 (2005) 10873–10882
polymer
www.elsevier.com/locate/polymer

Disruption of self-assembly and altered mechanical behavior in polyurethane/zinc oxide nanocomposites

Junrong Zheng[a,b,1], Rahmi Ozisik[a,c,*], Richard W. Siegel[a,c]

[a]*Rensselaer Nanotechnology Center, Rensselaer Polytechnic Institute, Troy, NY 12180, USA*
[b]*Department of Chemistry, Rensselaer Polytechnic Institute, Troy, NY 12180, USA*
[c]*Department of Material Science and Engineering, Rensselaer Polytechnic Institute, Troy, NY 12180, USA*

Received 18 May 2005; received in revised form 23 August 2005; accepted 31 August 2005
Available online 22 September 2005

Abstract

The addition of less than 1 vol%, 33 nm zinc oxide nanoparticles into a polyurethane matrix resulted in approximately 40% decrease in the Young's modulus, 80% decrease in strain at fracture, and 50% decrease in the storage modulus, but at the same time resulted in an ~11 °C increase in the glass transition temperature of the polymer. These results appear to contradict the general principle observed for many polymeric systems, where higher glass transition temperature generally means higher elastic modulus. Detailed experiments with FTIR, DMTA, FE-SEM, and AFM indicated that the addition of ZnO nanoparticles disrupts the phase separation in the polymer, resulting in weaker mechanical properties. The special interaction between the particles and polymer possibly constrains the mobility of polymer chains, which increases the glass transition temperature. The most likely reason for the disruption and the nature of the interaction is the reaction between the surface hydroxyl groups of the zinc oxide nanoparticles and the isocyanate groups of the polyurethane pre-polymer.

Keywords: Phase separation; Glass transition; Nanocomposite

1. Introduction

In recent years, polymer nanocomposites have attracted extensive research interests [1–5] around the world. It has been found that these materials have many advantages over traditional polymer composites with microscale fillers such as increased strength (without degrading other mechanical properties), decreased gas permeability, improved heat resistance, and enhanced electrical conductivity [1–4]. Special interest has been devoted to block copolymers filled with nanofillers [6–10] because it is possible to order nanofillers within the polymer matrix through self-assembly, thus creating highly organized hybrid materials. Block copolymers have different segments with different properties that can self-assemble to form phase-separated regular microdomains [9]. If one could make the fillers compatible with only one of the phases in the block copolymer, it would be possible to segregate the fillers into microdomains formed by this phase alone. Such spatially ordered materials could potentially be used in separation processes, catalysts, and photonic devices [6–8].

Although there have been some investigations [10–13] on the properties of thin films of diblock copolymers filled with nanoparticles that have alternating regions of polymer-rich and particle-rich domains, so far no systematic experimental studies have been undertaken to determine the factors governing the bulk morphology of the copolymer/nanofiller composites [9]. Most previous investigations [10–13] were concentrated on the effects of microdomains on the ordering of the fillers, while efforts to understand the effects of nanofillers on the phase-separation of the copolymers, to the best of our knowledge, have not yet been reported.

The present work addresses the effects of nanofillers on the phase separation of copolymers. As far as we know, this article may be the first to report how the nanofillers affect the bulk morphology of a copolymer and how such an effect changes the mechanical behavior of the polymer. The system we investigated consists of polyurethane (PU) and zinc oxide (ZnO) particles. PU is an important industrial material with

* Corresponding author. Address: Materials Science and Engineering, Rensselaer Polytechnic Institute, MRC-205, 110 Eight Street, Troy, NY 12180, USA.
E-mail address: ozisik@rpi.edu (R. Ozisik).
[1] Present Address: Department of Chemistry, Stanford university, Standford, CA 94305, USA.

0032-3861/$ - see front matter © 2005 Elsevier Ltd. All rights reserved.
doi:10.1016/j.polymer.2005.08.082

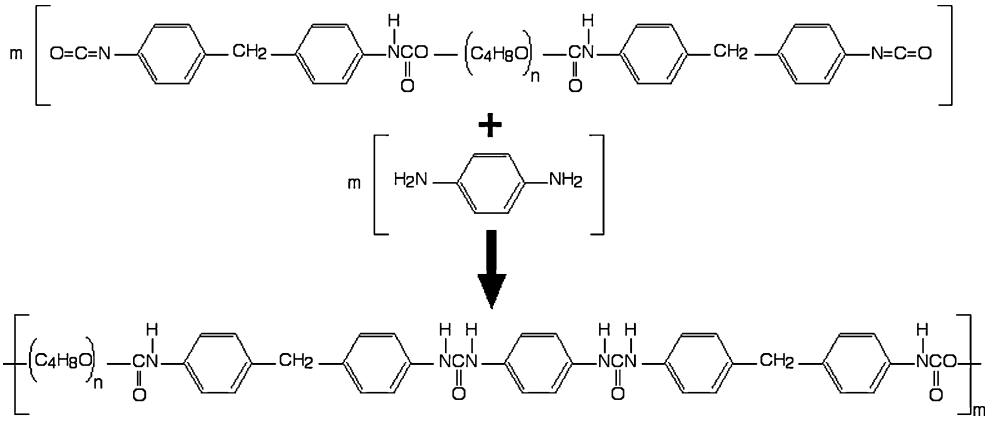

Fig. 1. Reaction scheme and chemical structure of polyurethane.

a wide range of applications [14,15]. It is a multiblock copolymer that forms phase-separated hard and soft segment domains [14]. A typical reaction scheme and chemical structure for a diamine cured PU with polyether as soft segments is shown in Fig. 1. The hard segment domains act as crosslinks and reinforcing agents [14]. Although many studies have been performed on PU/clay nanocomposites [16–21], most of them have been focused on the relationship between surface modification, exfoliation (or intercalation) of clay layers, and the mechanical properties. Because the exfoliation of clays is not a straightforward issue, different groups [16–19] obtained different mechanical properties, and none of these studies related the mechanical properties to the morphology changes of the copolymer. Compared to clays, ZnO particles are relatively easy to disperse, and compared to other particles such as aluminum oxide (Al_2O_3) or titanium dioxide (TiO_2), ZnO particles have almost no surface water [22], a factor that made ZnO our first choice. We added nano- and micro-scale ZnO particles into PU before the copolymer formation, and then used FTIR to monitor the reaction extent and functional group changes, AFM to measure the phase-separated micro-domains in both the neat PU and composites, FE-SEM to characterize the fracture surface (both cryogenic and ambient), and DMTA and tensile tests to measure the mechanical properties.

2. Experimental section

2.1. Sample preparation

The procedure we used to prepare PU composites was as follows: equal molar ratios of a degassed polyurethane pre-polymer (TDI-PPG pre-polymer with brand name Airthane® PPT-95A from Air Products with 6.32 wt% NCO) and a diamine curative (aromatic diamine with brand name Lonzacure® MCDEA curative from Air Products) were dissolved in purified THF to form a 15% solution (all mixtures are by weight) at 25 °C. ZnO particles (33 nm average size particles from Nanophase Technologies Corporation and 2.5 μm average size particles from Atlantic Equipment Engineers, both used as received) were dispersed in THF with a sonicator to form a 10% solution. The two solutions were combined and sonicated for 20 min in an ice/water bath. Subsequently, the mixture was concentrated to a 60% solution. The solution was cast into molds and cured at 40 °C for 8 h and then cured at 110 °C for 24 h to form films with thicknesses in the range of 0.2–3 mm. We prepared neat PU samples in the same way as the composites. In cured samples, the hard to soft segment ratio is 0.35:1 in weight.

In general, the common preparation procedure involves melt mixing [23], but it was found that because the pot-time was very short (about 1 min), it was very difficult to disperse the curative at the molecular level into the pre-polymer, which affected the results of the experiments (the storage modulus of the sample prepared with melt mixing was about 10–20% of that of the sample prepared with solution mixing at the same molar ratio of pre-polymer and curative). The solution mixing method described above was developed to make sure that the curative was well mixed with the pre-polymer at the molecular level. One concern about this procedure was whether the solvent was completely removed from the final product. To answer this question, one cured sample (1 mm in thickness) was put in an oven and heated under vacuum at 120 °C for 48 h. Samples with and without such a treatment were analyzed by TGA, FTIR and DMTA. No differences were observed between these two samples, which meant that the solvent had been successfully removed to an acceptable level.

To choose a suitable curing time, FTIR was used to monitor the reaction extent. The intensity of the isocyanate peak at $\sim$2270 cm^{-1} was followed for samples cured for varying durations and it was found that 24 h is a suitable time. After 24 h, the isocyanate peak almost completely disappears and its intensity does not change.

3. Measurements

3.1. Atomic force microscopy

The AFM (Autoprobe CP, Park Scientific Instruments, with tip, ultralevel D, spring constant $\sim$18 N/m; and Multimode Scanning Probe Microscope from Digital Instruments) measurements were conducted at room temperature using

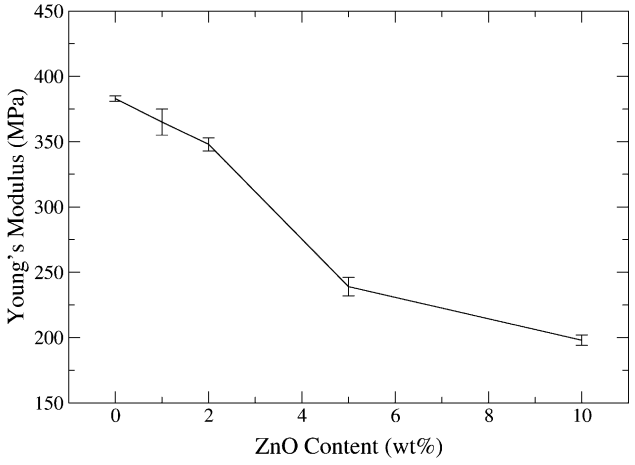

Fig. 2. Young's modulus of polyurethane and nanocomposites with 33 nm ZnO at room temperature.

the tapping mode with different forces. The samples analyzed were neat PU and the composites with 5%, 33 nm ZnO with two different film thickness values: ~500 μm (prepared from 60% THF solution) and <1 μm (prepared from 10% THF solution), formed by spin coating at 3000 rpm on silicon wafers.

3.2. Field emission scanning electron microscopy

Fractographs were observed with an FE-SEM (JEOL JSM-6330F Field Emission SEM). Samples were prepared in two ways: (i) for cryogenic fracture, samples (~0.5 mm thick) were dipped into liquid nitrogen for 20 min and then broken (bending mode) in liquid nitrogen with two pliers, and (ii) for ambient fracture, pre-notched samples (~0.5 mm thick) were torn (tensile mode) until they fractured at room temperature (~21 °C). All samples were coated with a layer of gold or platinum before SEM characterization.

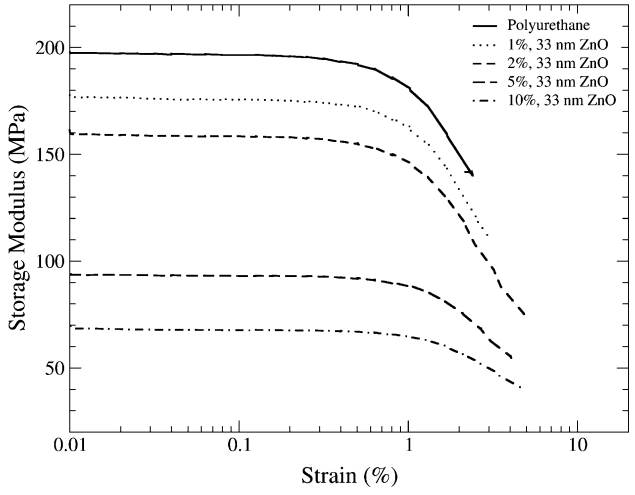

Fig. 3. Storage modulus of polyurethane and nanocomposites with varying 33 nm ZnO content from DMTA tests at room temperature.

Table 1
Results of the tensile and dynamic mechanical (DMTA) tests

Sample	T_g (°C)	G' (MPa)	E (MPa)	Strain at fracture
Polyurethane	−2.9	196	383±2	7.5±1.0
PU with 1%, 33 nm	0.7	176	365±10	4.7±0.4
PU with 2%, 33 nm	4.7	158	348±5	3.3±0.3
PU with 5%, 33 nm	8.3	93	239±7	1.16±0.2
PU with 10%, 33 nm	11.2	68	198±4	0.85±0.1
PU with 5%, 2.5 μm	−2.1	191	381±5	5.8±0.5
PU with 5%, 33 nm ZnO modified with Si3	−0.8	169	402±10	5.8±0.5

The dynamic mechanical tests were performed at a frequency of 1 Hz and 0.1% strain. T_g, glass transition temperature; G', storage modulus; E, Young's modulus. Composites are in weight percentage.

3.3. Fourier transform infrared spectroscopy

FTIR (Perkin Elmer Paragon 1000) measurements were conducted at room temperature in the transmission mode. The thin films for FTIR measurements were prepared in the same way as described in the AFM section for the thinner samples.

3.4. Dynamic mechanical thermal analysis and tensile tests

The mechanical responses of samples were measured with a DMTA (DMTA V, Rheometric Scientific) and an Instron 8562. Two kinds of DMTA measurements (both at 1 Hz, 6.2832 rad/s) were performed: (i) dynamic strain sweep at room temperature (21 °C) and (ii) dynamic temperature ramp sweep at 0.1% strain and 2 °C/min from −130 to 200 °C. Tensile tests were performed to obtain the Young's modulus and strain at fracture of samples at room temperature and at

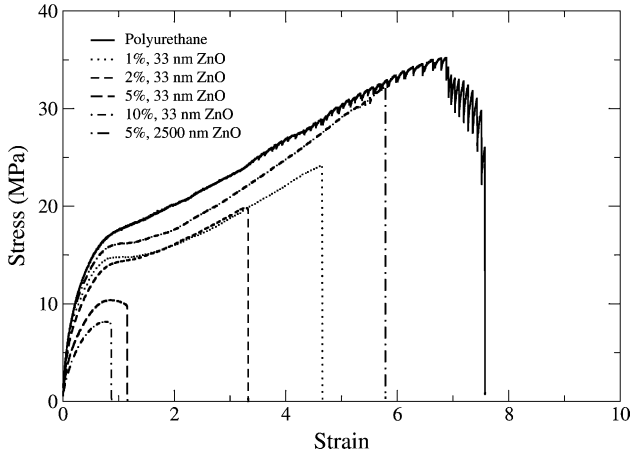

Fig. 4. Stress–strain curves of polyurethane and composites with varying ZnO content as obtained from tensile tests at room temperature.

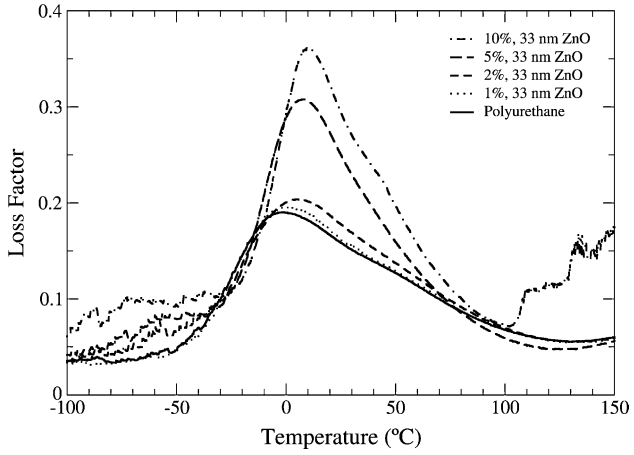

Fig. 5. Loss factor values versus temperature of polyurethane and nanocomposites with varying 33 nm ZnO content obtained from the DMTA tests. (a) The peak position indicates T_g.

the rate of 10 mm/min. The neck dimension of the sample for tensile tests is $2.7\times2.8\times13$ mm^3. Each data point is averaged from 3–6 samples.

4. Results and discussion

4.1. Mechanical/thermal analysis

The results of the tensile tests are presented in Fig. 2 and the DMTA tests are presented in Fig. 3 (Table 1). All tests were performed at room temperature (~21 °C). Figs. 2 and 3 clearly show that both the Young's modulus and the storage modulus decrease with increasing 33 nm ZnO content, whereas for the microcomposite (2.5 μm ZnO), both moduli remain similar to those of neat PU. For the composite system with 5% (less than 0.8 vol%) 33 nm ZnO, the Young's modulus and storage modulus decreased approximately 38 and 52% (at the linear region) compared to pure PU, respectively. A more dramatic change is observed in the strain at fracture shown in Fig. 4. The strain at fracture for neat PU is around 750%, whereas it is only around 120% for the nanocomposite with 5%, 33 nm ZnO. These results are somewhat confusing because addition of nano-size ZnO results in a decrease in both modulus and strain at fracture.

The changes in mechanical properties of nanocomposites discussed above do not result from the stoichiometry change caused by ZnO nanoparticles, although changing stoichiometry [14, 23] can affect the mechanical properties of PU. Our experiments show that the mechanical properties of the neat polymer samples with different stoichiometries (±6%) are the same. Adding 10% of 33 nm ZnO nanoparticles can at most change the polymer stoichiometry 6%, assuming there are 1% surface hydroxyl groups on the particles and all these groups can act as curatives. In fact we did not detect any surface water for ZnO particles with TGA [22].

Because the Young's and storage moduli of the composites decreased with increasing ZnO nanoparticle content, the glass transition temperature (T_g) of the polymer was expected to also decrease. For a typical homopolymer, T_g is inversely proportional to polymer chain mobility—low chain mobility results in high T_g and also means that it is harder to deform the polymer, therefore a higher modulus is expected. Our experimental findings showed an opposite result: the composite with high ZnO nanoparticle content had a low modulus, but

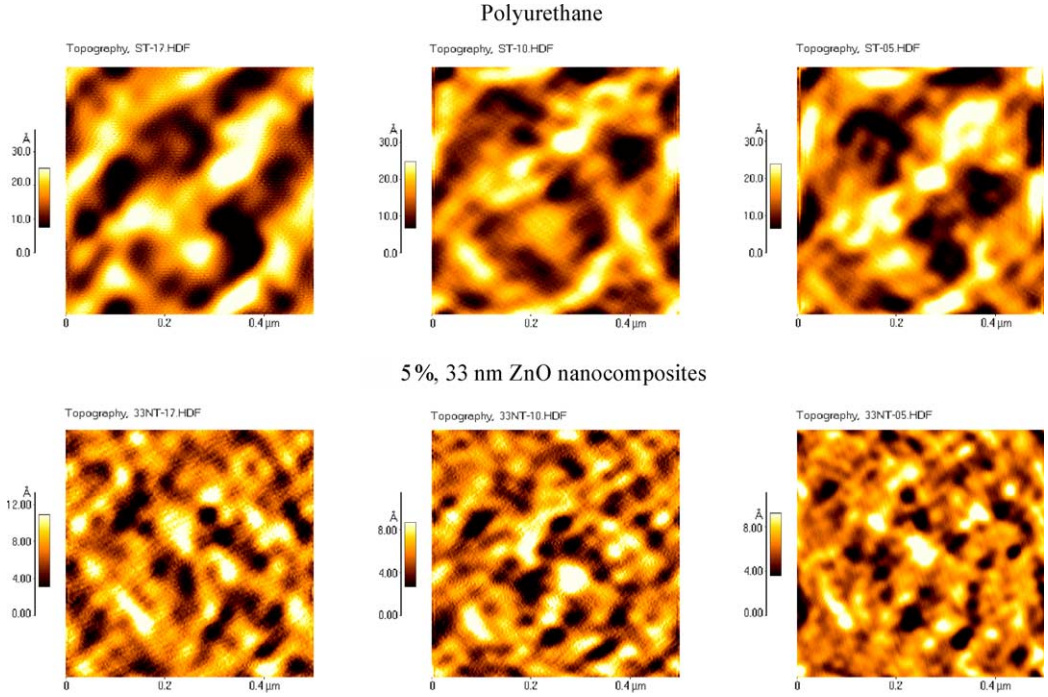

Fig. 6. AFM topographs of polyurethane and nanocomposites with 5%, 33 nm ZnO. The size of all images is 500×500 nm^2. Tapping force increases from left to right. Figures in the same column were taken under the same conditions.

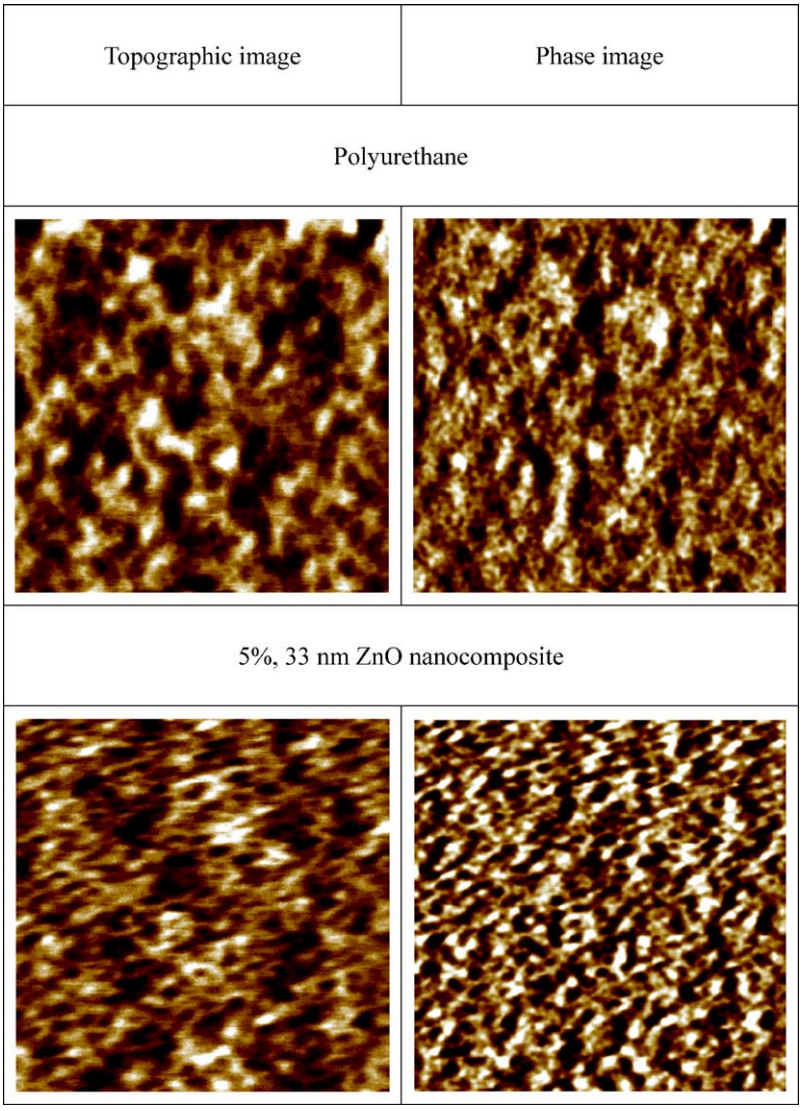

Fig. 7. Topographic and phase images from polyurethane and 5%, 33 nm ZnO nanocomposite (1000×1000 nm^2).

a high T_g, as shown in Fig. 5. The peak position around 0 °C represents the T_g of the PU soft segments [14] (Table 1). The intensity of the peak increases with higher ZnO nanoparticle content, which means that the elasticity of the PU is weakened by adding ZnO nanoparticles, consistent with the tensile test results.

A possible explanation for these apparently conflicting results may be due to the phase separation of PU. In PU, there are two distinct phases—hard and soft phases. The hard phases act as reinforcing fillers and deformable physical crosslinking points. It is probable that adding ZnO nanoparticles disrupts the phase separation of PU such that there are fewer hard phases formed in the composites (compared to neat PU) because of some special interactions (most likely the reaction between the prepolymer and the surface hydroxyl groups of the nanoparticles) between the polymer and the ZnO nanoparticles. Because of these interactions, each nanoparticle can act as a crosslinking point, which constrains the polymer chain mobility and, thus, limits the formation of the phases. This would lead to less hard phase formation and, therefore, to a lowered modulus. The formation of the crosslinks between the nanoparticles and the polymer leads to a higher T_g and a smaller strain at fracture. Some supporting data for this explanation are given in the following sections.

4.2. Morphology

4.2.1. Atomic force microscopy

Atomic force microscopy (AFM) was used to study the morphology of PU and its composites. Transmission electron microscopy (TEM) was not used because TEM studies on stained films [24, 25] have yielded some insight, but the experiments are limited by the efficacy of staining, type of PU, and the possibility of electron beam damage. In recent years, AFM has been used to image the microdomains in PU [26–28]. The mechanical properties (such as hardness and modulus) of the hard domains and the soft domains are quite different, and such differences can be translated into a force difference in

AFM tapping mode measurements, and hence an image of the morphology (showing the hard and soft domains) can be formed.

Fig. 6 shows AFM images of neat PU (top) and composites (bottom) containing 5%, 33 nm ZnO particles. The tapping force increases from left to right and the images in the same column were recorded under the same measuring conditions. It can easily be seen that the size of the hard domains (the bright regions) of the neat polymer are much larger than those of the nanocomposite. The AFM images reflect the phase difference rather than surface roughness. McLean et al. [27] found that for thermoplastic PU, the AFM topographical and phase images are quite similar because of a thin and flat soft-segment layer that covers the first few Ångstroms of the surface due to its lower surface energy compared with the hard segments.

We also recorded the topographic and phase data at the same time with another AFM (Multimode Scanning Probe Microscopy, Digital Instruments) to see if there is any difference between these two kinds of data for our systems. The topographic and phase images are similar (Fig. 7), but it seems that the phase images give more information about the surface morphology. Looking at the neat PU images in Fig. 7, we suggest two levels of hierarchy for self-assembly of the phase separation: (i) the hard segments of our thermoset PU form hard domains of about 10 nm in width, which are similar to McLean's results [27] in thermoplastic PU, and (ii) these hard domains self-assemble to form larger microdomains of about 100–400 nm in length and about 50 nm in width. In the case of the 5%, 33 nm ZnO composites, the hard segments also formed hard domains, but the number of these hard domains is less than that in the neat PU. Furthermore, the hard domains cannot self-assemble to form larger microdomains. We believe that this change in microstructure of the nanocomposite is the key reason for the observed changes in mechanical properties.

The AFM images shown in Fig. 7 were obtained using thick films ($\sim$500 μm), and are quite different from those of McLean [27]. To make a comparison, thin films were prepared by spin coating. These images are shown in Fig. 8. In this case, $\sim$10 nm thick lamellae [27] can be clearly seen in Fig. 8(A), but the self-assembly into larger scale phases is not seen. This is also consistent with our observations in mechanical tests: when samples are thinner than a certain thickness, thinner samples give weaker properties. We can immediately see that in the composite, the number and the length of the lamellae are much smaller than those in the neat PU. These images confirm our suggestion that the addition of ZnO nanoparticles disrupts the phase separation in PU.

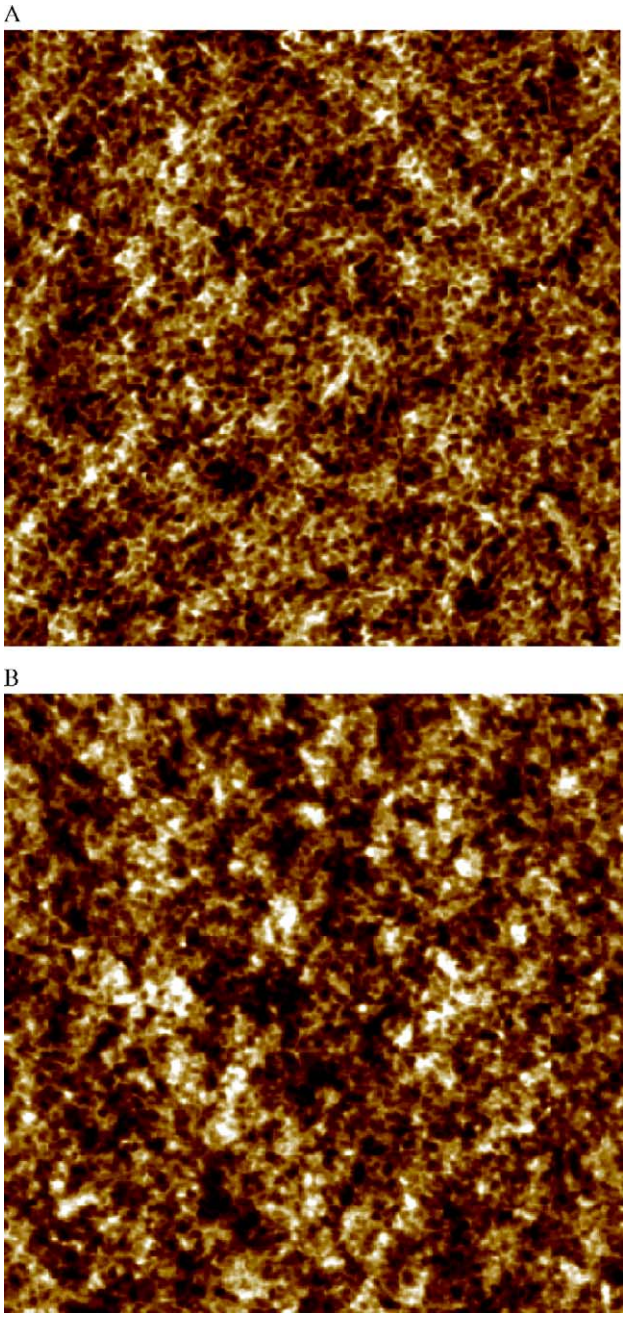

Fig. 8. AFM topographs ($1000\times1000\ nm^2$) of polyurethane (A) and nanocomposite with 5%, 33 nm ZnO (B) in thin films obtained by spin coating. Maximum height difference in topographic images is 5 nm (A) and 4 nm (B).

4.2.2. Scanning electron microscopy

SEM was used to characterize the particle dispersion and fracture surfaces of neat PU and the PU composites containing 10% micron-size (2.5 μm) and 5% nano-size (33 nm) ZnO particles under two conditions: (i) cryogenic fracture (-193 °C, well below the T_g of the soft segments), and (ii) ambient fracture (21 °C, above the T_g of the soft segments).

The crack growth regions (cryogentic fracture) are shown in Fig. 9(A) for the microcomposite. Similar regions were found in the neat PU and nanocomposites. These regions are quite similar to those found in glasses and ceramics [29] with three typical subregions: (i) a smooth region called mirror, (ii) small radial ridges called mist, and (iii) rough ridges called hackle [29]. In general, these three regions are caused by the propagation of a pre-existing flaw subsequent to the application of a critical stress, and the radius of the mirror ring is related to the applied stress [29]. A detailed mechanism of the formation of such a morphology is still unknown [29].

By comparing the SEM images, an obvious difference can be seen between the neat PU and the nanocomposites:

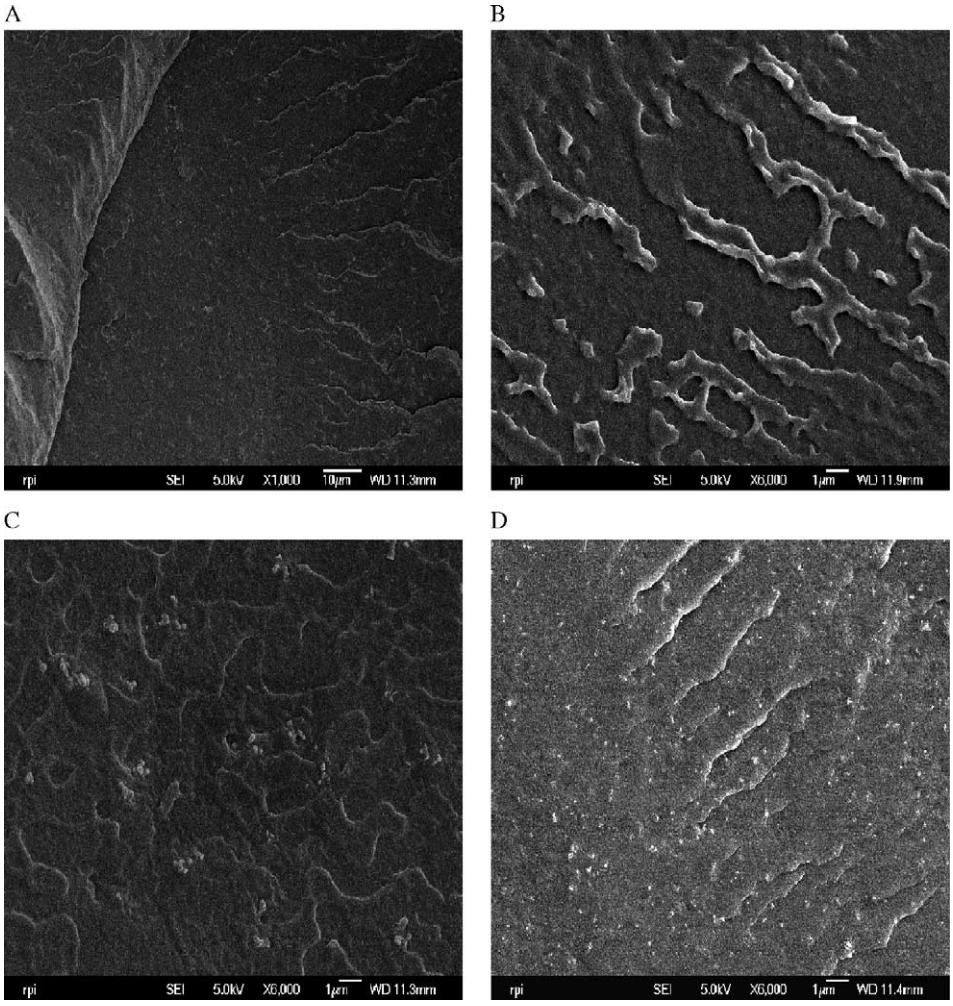

Fig. 9. Cryogenic fractographs of polyurethane and composites. (A) Image of microcomposite with 10% ZnO microparticles showing the three regions: mirror, mist, hackle. (B) Mirror region of the neat PU showing clear patches. (C) Mirror region of the microcomposite showing clear patches. (D) Mist and mirror regions for the nanocomposite with 5% ZnO nanoparticles. X-axis lengths: (A) 117 μm, (B)–(D) 19.5 μm.

the mirror region of the neat PU and the microcomposite contain some 'patch' patterns (Fig. 9(B) and (C)), whereas the mirror region of the nanocomposite is very smooth (left lower corner in Fig. 9(D)). These pictures suggest that adding nanoparticles into the PU somehow changes the fracture behavior of the polymer. The detailed mechanism for the change is unknown. The following is our tentative explanation. In general, patch patterns in polymer fracture surfaces are believed to form during brittle, unstable fracture in glassy polymers [30]. During brittle, unstable fracture, craze breakdown occurs primarily by fibril-matrix separation along the interface between crazed and non-crazed material at the upper or lower craze edges. This process results in a patchwork structure of the residual craze matter on the final fracture surface. Crazing is a mode of localized plastic deformation that occurs particularly in glassy polymers subjected to tensile stresses. It involves orientation of molecular chain segments in the direction of the principal stress together with cavitation or void formation [31]. It is possible that in the neat PU and microcomposites, the stress is distributed unevenly in the samples during fracture, due to the large microphase separation, which results in obvious patterns in the mirror region. On the other hand, in the nanocomposites, the microphase separation is much smaller and leads to a more even stress distribution, resulting in a smoother mirror region. Experimentally, it was also found that the nanocomposites are easier to fracture and more brittle than the neat PU and microcomposites in liquid nitrogen.

Images shown in Fig. 10 are ambient fractographs of the neat PU and the composites. These images are totally different from those obtained by cryogenic fracture—the surfaces are much flatter and smoother. There are also some differences between the ambient fractographs of the neat PU and the composites. The surface of the neat PU is the smoothest, while the surface of the microcomposite is comparatively smooth except for some pores, and the surface of the nanocomposite is the roughest. Again, the detailed mechanism for these behaviors is unknown. Our tentative explanation is as follows. The reason for the smooth fracture surface for PU is that the soft phase is energetically favored [27] so that this phase will automatically rearrange to cover the fracture surface driven by the surface energy. This

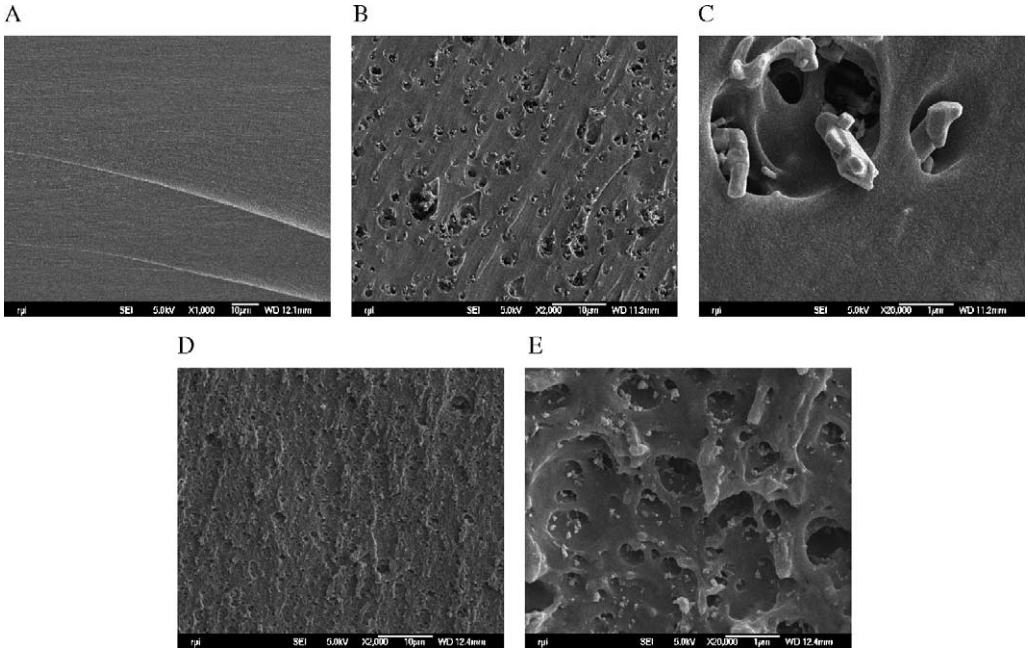

Fig. 10. Ambient fractographs of polyurethane and composites. (A) Neat polyurethane; (B) and (C) are composites with 10%, 2.5 μm ZnO particles; and (D) and (E) are nanocomposites with 5%, 33 nm ZnO particles. X-axis lengths: (A) 117 μm, (B) and (D) 58.5 μm, (C) and (E) 5.85 μm.

rearrangement does not happen during cryogenic fracture because the temperature is lower than T_g and the polymer chains are frozen. The rough fracture surface of the nanocomposites results from smaller phase separation and the special interaction between the nanoparticles and the polymer that constrains the polymer chains' mobility and the efficiency of the rearrangement. As shown above, the fracture surfaces of the nanocomposites are different from that of the neat PU: rougher above T_g, and smoother below T_g. The behaviors are probably caused by the change of phase separation in the nanocomposites.

4.3. Particle/polymer interface

In the previous sections , we have suggested that addition of ZnO nanoparticles changes the microstructure of the PU, and that the reason for such an effect is probably the special interactions between the nanoparticles and the PU—a possible reaction between the nanoparticles and the PU pre-polymer. Here, we give data to support this claim using Fourier transform infrared spectroscopy (FTIR).

Fig. 11 shows the FTIR results on ZnO particles (2.5 μm and 33 nm) after being treated with PU prepolymer. The treatments were performed under the same conditions as those for the composite preparation: particles and the pre-polymer were mixed in THF and sonicated at 0 °C for 20 min, then the particles were separated from the solution and cleaned by centrifuging for three times, and the separated particles (products) were cured at 110 °C for 24 h under vacuum. As shown in Fig. 11, we did not see any difference in ZnO microparticles before and after being treated with the pre-polymer. On the other hand, the signals are quite different for the nanoparticles. After the treatment with pre-polymer, several new peaks appeared in the FTIR data. The peak around 3000 cm^{-1} belongs to C–H stretching, and the peak around 3500 cm^{-1} belongs to free N–H stretching [17] (no hydrogen bonding; in polymer, the N–H peak is around 3300 cm^{-1} due to hydrogen bonding as shown in Fig. 12). The C–H stretch peak (3000 cm^{-1}) is similar to that of the PU prepolymer, which means that the prepolymer is attached to the surface of the nanoparticles. The free N–H stretch peak (3500 cm^{-1}) is new, which is absent in the prepolymer. The most likely explanation for the formation of the new N–H groups is that they are the reaction products between the surface hydroxyl groups of the nanoparticles and the isocyanate groups of the prepolymer. The other support for this argument comes from the color change that was observed: the reacted particles turn to pale yellow from pure white whereas the prepolymer is transparent.

Fig. 12 shows the FTIR results for PU and the nanocomposite with 5%, 33 nm ZnO particles cured at 110 °C for 24 h. There is no difference between the two spectra (since the amount of hydroxyl groups on the ZnO surface is small compared to the amount on the pre-polymer) except for one peak around 500 cm^{-1} in the nanocomposite that belongs to the ZnO particles. From Figs. 11 and 12, it is seen that the N–H stretching [17] for the reacted particles is around 3500 cm^{-1}, whereas it is around 3300 cm^{-1} for the PU and the nanocomposite. We do not see a clear peak for the free NH in the composite spectrum because the free NH is only at most 2% (estimated from $<$ 1% hydroxyl group on the nanoparticles) of the hydrogen bonded ones, and the transition dipole moment of the free NH is smaller than that of the hydrogen bonded one. The difference is caused by hydrogen bonding. In the reacted nanoparticles, the NH groups are constrained by the ZnO

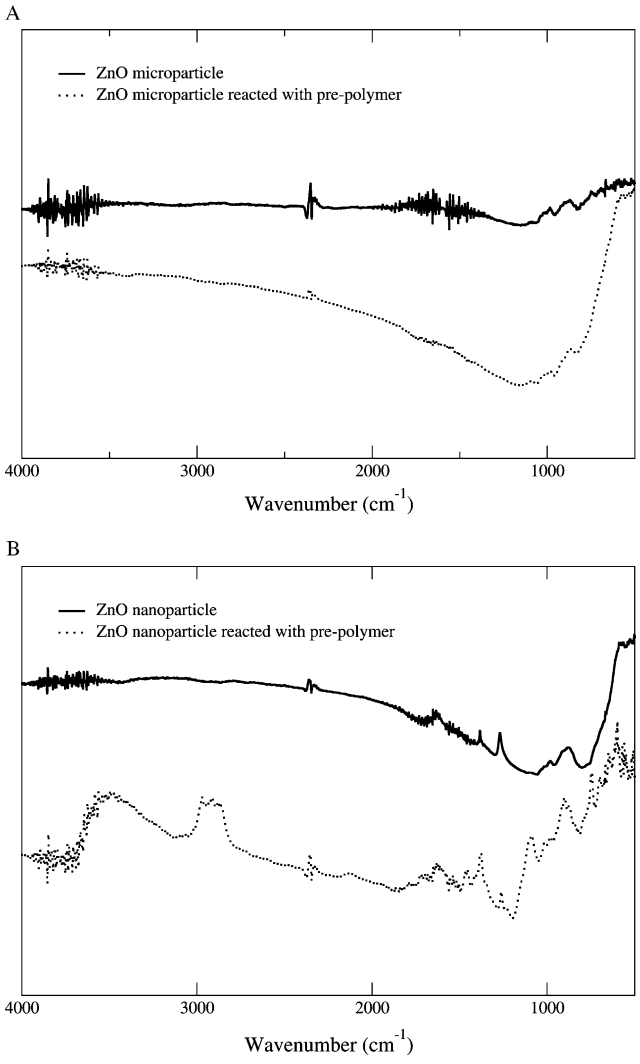

Fig. 11. FTIR spectra showing the results of treatments on the ZnO particles with PU prepolymer (A) 2.5 μm ZnO particles or (B). 33 nm ZnO.

surface geometry and thus cannot form hydrogen bonds; therefore N–H stretching appears at a higher frequency in the IR spectrum. This observation shows that ZnO nanoparticles constrain the chain mobility, which is consistent with the DMTA measurements of higher T_g in nanocomposites. On the other hand, in the neat polymer and nanocomposite, polymer chains are flexible and NH groups can easily find a carbonyl group to form hydrogen bonds to stabilize the system.

4.4. Modification of the surfaces of ZnO nanoparticles

The results of the experiments indicate that the mechanical properties of PU/ZnO nanocomposites change probably due to changes in the microphase separation caused by the special interaction between the PU and nanoparticles—most probably due to a reaction between the surface hydroxyl groups on ZnO nanoparticles and the pre-polymer. Deducing from this conclusion, it can be predicted that there should be no obvious

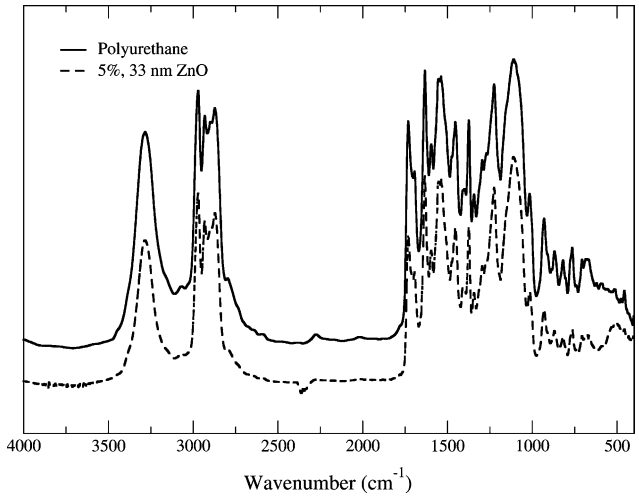

Fig. 12. Results of the FTIR performed on polyurethane and the composite with 5%, 33 nm ZnO particles cured at 110 °C for 24 h.

difference in the mechanical properties between neat PU and nanocomposites if the surface hydroxyl groups are removed from the particles. Therefore, the following experiments were performed to test this assumption. The 33 nm size ZnO particles were coated with $SiCl_3C_{12}H_{23}$ (Si3) to cover most of the hydroxyl groups on the ZnO surface (the surface hydroxyl groups react with the silane to form Zn–O–Si bonds), and a 5% nanocomposite was prepared using these modified particles and analyzed by tensile tests and DMTA. The results of these tests are shown in Fig. 13 and Table 1. It is clearly seen that the composite prepared with coated ZnO nanoparticles, the microcomposite (prepared with 2.5 μm ZnO particles), and the neat PU have similar properties, whereas the uncoated ZnO nanocomposite has very different properties. The difference between the uncoated nanocomposite and microcomposite arises due to the low surface area of the ZnO particles in the microcomposite system (compared to the ZnO nanoparticles), which leads to very little bonding between the hydroxyl groups

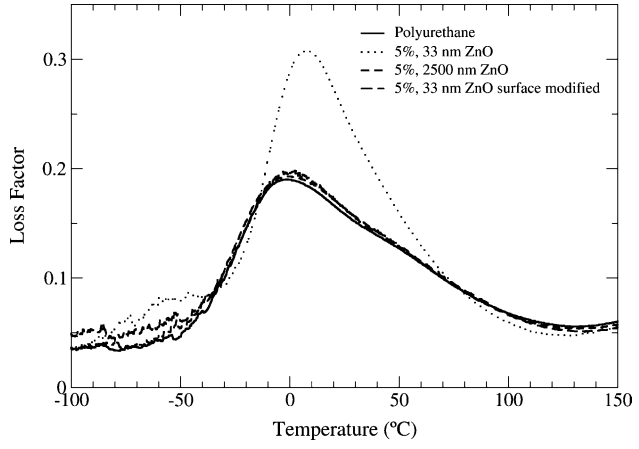

Fig. 13. Loss factor values versus temperature of polyurethane and various composites with 5% ZnO particle content. The peak position indicates T_g.

and the pre-polymer. The coated ZnO composite behavior is similar to the microcomposite because the hydroxyl groups are removed by surface treatment.

It should be pointed out that in block copolymer nanocomposites, forming covalent bonds between the polymer and the fillers is not necessarily the only reason for the disruption of the microphase separation. This issue will be addressed in our next publication discussing the effects of different fillers and interactions on the properties of the composites. In the current ZnO/PU system, experiments do support that a reaction takes place between the prepolymer and the nanoparticles.

5. Conclusions

Based on our experimental results, the following conclusions can be made:

1. Adding ZnO nanoparticles decreases the modulus and strain at fracture, and increases the glass transition temperature of the polyurethane.
2. A small amount of ZnO nanoparticles can weaken and change the mechanical properties of PU significantly due to the disruption of the phase separation in the polyurethane.
3. The reaction between the hydroxyl groups that are present on the ZnO nanoparticles and the isocyanate groups is a very likely reason for the disruption of the phase separation.

These results pose an interesting question that needs further study: Is it possible to control the properties of block copolymers by controlling their phase separation through addition of nanoparticles with controlled and well-defined surfaces? We will explore this in our future work.

Acknowledgements

Financial support from Albany International Corporation and the Nanoscale Science and Engineering Initiative of the National Science Foundation under NSF award number DMR-0117702 is gratefully acknowledged. The authors would like to thank Benjamin Ash for his help in DMTA measurements, Fu Tang for his help in AFM measurements, and Zhizhong Wu for his help in purifying THF. The helpful discussions with Chunzhao Li are also appreciated.

References

[1] Alexander M, Dubois P. Mater Sci Eng Rev 2000;28:1.
[2] Balazs AC. Curr Opin Colloid Interface Sci 2000;4:443.
[3] Giannelis EP. Appl Organomet Chem 1998;12:675.
[4] Soo PP, Huang BY, Jang YI, Chiang YM, Sadoway DR, Mayers AM. J Electrochem Soc 1999;146:32.
[5] Kojima Y, Usuki A, Kawasumi M, Okada O, Fukushima Y, Kurachi T, et al. J Mater Res 1993;8:1185.
[6] Templin M, Franck A, DuChesne A, Leist H, Zhang YM, Ulrich R, et al. Science 1997;278:1795.
[7] Zhao D, Feng J, Huo Q, Melosh N, Fredrickson GH, Chmelka BF, et al. Science 1998;279:548.
[8] Chan VZH, Hoffman J, Lee VY, Iatrou H, Avgeropoulos A, Hadjichristidis N, et al. Science 1999;286:1716.
[9] Thompson RB, Ginzburg VV, Matsen MW, Balazs AC. Macromolecules 2002;35:1060.
[10] Morkved TL, Wiltzius P, Jaeger HM, Grier DG, Witten TA. Appl Phys Lett 1994;64:422.
[11] Zehner RW, Lopes WA, Morkved TL, Jaeger HM, Sita LR. Langmuir 1998;14:241.
[12] Fog DE, Radzilowski LH, Blanski R, Schrock RR, Thomas EL. Macromolecules 1997;30:417.
[13] Fog DE, Radzilowski LH, Dabbousi BO, Schrock RR, Thomas EL, Bawendi MG. Macromolecules 1997;30:8433.
[14] Hepburn C. Polyurethane elastomers. Essex, England: Elsevier Science; 1992.
[15] David DJ, Staley HB. Analytical chemistry of the polyurethanes. vol. XVI. NY, USA: Wiley; 1969 [part 3].
[16] Zilg C, Thomann R, Mulhaupt R, Finter J. Adv Mater 1999;11:49.
[17] Tien YI, Wei KH. Macromolecules 2001;34:9045.
[18] Wang Z, Pinnavaia TJ. Chem Mater 1998;10:3769.
[19] Chang JH, An YU. J Polym Sci, Part B: Polym Phys 2002;40:670.
[20] Tortora M, Gorrasi G, Vittoria V, Galli G, Ritrovati S, Chiellina E. Polymer 2002;43:6147.
[21] Yao KJ, Song M, Hourston DJ, Luo DZ. Polymer 2002;43:1017.
[22] Zheng J, Siegel RW, Toney CG. J Polym Sci, Part B: Polym Phys 2003;41:1033.
[23] Beck RA, Truss RW. Polymer 1999;40:307.
[24] Li C, Cooper SL. Polymer 1990;31:3.
[25] Schrader S, Li X, Guo F, Liu Y, Luo J, Xu D. Macromol Chem Rapid Commum 1988;9:597.
[26] Garrett JT, Siedlecki CA, Runt J. Macromolecules 2001;34:7066.
[27] McLean RS, Sauer BB. Macromolecules 1997;30:8314.
[28] Takahashi A, Kita R, Kaibara M. J Mater Sci 2002;13:259.
[29] Mecholsky JJ, Freiman SW. In: Freiman SW, editor. Fracture mechanics applied to brittle materials. CA, USA: American Society for Testing and Materials; 1979. p. 136 [ASTM STP 678].
[30] Friedrich K. Adv Polym Sci 1983;52/53:225.
[31] Sauer JA, Chen CC. Adv Polym Sci 1983;52/53:169.